ADVANTAGES OF SILICON PHOTON COUNTERS IN GATED MODE

APPLICATION NOTE

Matthieu Legré(1), Tommaso Lunghi(2), Damien Stucki(1), Hugo Zbinden(2)

(1) *ID Quantique SA, Rue de la Marbrerie, CH-1227 Carouge, Switzerland*

(2) *Group of Applied Physics, University of Geneva, CH-1211 Geneva, Switzerland*

Abstract

We present gated silicon photon detectors based on two commercially available avalanche photodiodes (APDs) and one customised APD from ID Quantique SA. This customised APD is used in a commercially device called id110. A brief comparison of the two commercial APDs is presented. Then, the charge persistence effect of all of these detectors is presented for several photon levels.

Introduction

Silicon single-photon avalanche diodes (Si SPADs) are a standard solid-state solution for single-photon detection in the visible and near-infrared [1]. In particular, Si SPADs can attain high photon-detection efficiencies and extremely low dark-count rates. The structure based entirely on silicon has only a limited number of traps in the multiplication region, resulting in a device that is not much affected by afterpulsing. Thus, Si SPADs are normally used in free-running mode. However, recently the advantages of gating a thin Si diode have been explored for near-infrared spectroscopy experiments [2, 3].

Here we take two general situations, which have been defined in [4], back where a gated Si detector shows some essential advantages:

(a) Detecting a photon hidden in continuous faint light : in this scenario (figure 1(a)) the detector is continuously illuminated by faint light. The time interval between two subsequent photons is, on average, smaller than the dead time of the detector. The photons of interest are hidden in the beam but their arrival times are known. Under these conditions, a free-running detector is saturated or even blinded, reducing the detection probability. This situation can be found in quantum-cloning [5] and faithful swapping [6] experiments.

(b) Detecting a photon arriving after a strong pulse: in this scenario (figure1(b)) a strong pulse impinges on the detector before the arrival of the photon of interest. Hence, when the photon of interest arrives, a free-running detector is either in its dead time or its noise is highly increased by afterpulsing. In addition, the strong pulse can induce additional noise generated by an effect called charge persistence [7, 8]. This situation can be found in Optical Time Domain Reflectometry [9], in fluorescence spectroscopy [2, 3] as well as in quantum-memory experiments which require strong preparation pulses [10].

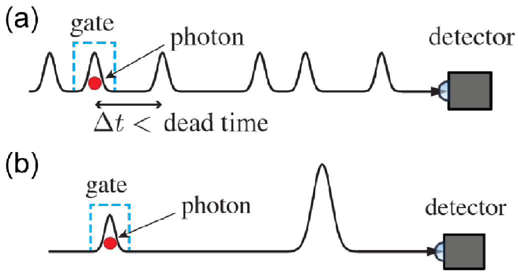

Figure 1 : the experimental scenari where a gated detector pays an essential role. (a): applying a gate ensures that the detector is active when the photon of interest arrives, even if the detector is constantly being illuminated. (b): applying a gate ensures that the detector is not blinded by the preceding strong pulse.

Commercial diodes

Two commercially available APDs have been used to implement our single photon detection module working in gated mode. We will call them APD-1 and APD-2. Both APDs have an active area diameter of 500um and a thick junction. This quite large diameter makes the dark count rate and the internal capacitance of those diodes quite large compare to the same parameters of smaller diodes. This means that the single photon modules based on those diodes have a higher noise and a longer dead time compare to modules with smaller APD. The typical value of the dead time given by the providers for those APDs is between 500ns and 1us depending on the quenching resistor which is used. Hence, the module is blinded or inactive for a quite long time period after detections. This makes the gated mode quite relevant for such diodes in the case **(a)** described previously.

In addition to those two diodes, we characterize a silicon APD with a thin junction and an active area diameter of 100um. This APD has been designed and produced by ID Quantique. It is a pigtailed APD with a 105um diameter core MMF fibre.

Electrical circuits

Because the breakdown voltage values of the three diodes are strongly different, two electrical circuits have been developed. The first one generates electrical gate with huge amplitude to drive the thick junction APD. The second one is dedicated to thin junction diodes.

Electrical circuit for thick junction APD (or high breakdown voltage)

This electrical circuit has been deeply detailed in [4]. A scheme of its principle is depicted in figure 2. The electrical gates are generated by an Avtec pulser (AVI-MP-N). It allows the generation of gate amplitude up to 40V with a rising time shorter than 2ns. The electrical spikes that occur when the electrical gate is applied on the APDs have amplitude of about 7V. Hence, an auxiliary line composed of one resistor and one capacitance identical to the internal ones of the APDs is used to strongly reduce those spikes. In the following sections, the pulse width of the pulser has been set to 20ns.

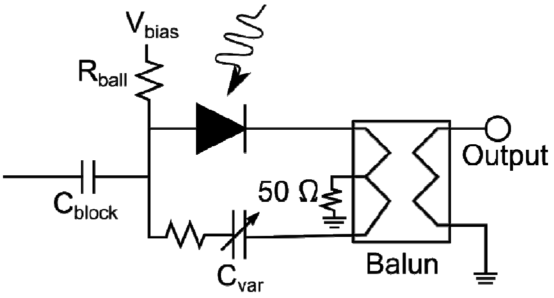

Figure 2 : scheme of the electrical circuit used for thick junction APDs.

Electrical circuit for thin junction APD (or high breakdown voltage)

This electrical circuit is a modified version of the one used in a product from ID Quantique called id210 [11]. This electrical circuit allows one to generate gate amplitude of 5-6V which is sufficient for thin junction APD. This electrical circuit has been included in the same platform than the id210. This new module is now commercially available and is called id110 [12]. A picture of the id110 is shown in figure 3.

Figure 3: picture of the id110 (ID Quantique product)

Electrical signals

In figure 4, we can see the electrical signal coming out from the Balun of the electrical circuit for thick junction APD when an electrical gate is applied but no avalanche occurs. The strong spikes have been reduced to spikes with amplitude of 0.1V and 0.4V for the APD-2 and APD-1 diodes respectively. We spent time to reduce the spikes, but we didn't try to perfectly compensate for them, so we don't claim that APD-1 are more difficult to compensate than the APD-2 ones. The spike levels shown in figure 6 are sufficient for us to work with those diodes because, as can be seen in figure 5, the output electrical signal corresponding to an avalanche is much higher than the residual spikes.

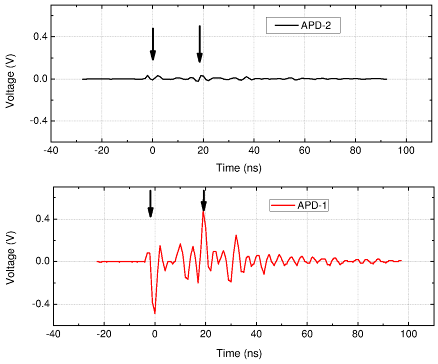

Figure 4: Output signal coming out from the balun when no avalanche occurs

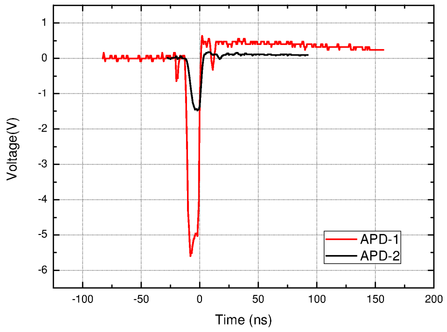

Figure 5 : Output signal coming out from the balun when an avalanche occurs

Efficiency vs. noise

The first measurement which has been performed on the gated modules is a noise vs. efficiency characterization. APD-2 diode has a thinner junction than the junction of APD-1. So APD-2 has a higher efficiency value for near infrared light, whereas APD-1 diode is more efficient around 600nm. That's the reason why we characterize the diodes at both wavelengths: 655nm and 808nm. The results of the measurements are shown in figure 6 and 7. As expected, at a given excess voltage value the APD-1 is more efficient than the APD-2 at 655nm. This is the opposite situation at 808nm. With an excess voltage of 10V, the efficiency values of the APD-1 are 64% at 655nm and 37% at 808nm. With an excess voltage of 20V, the efficiency values of the APD-2 are 60% at 655nm and 64% at 808nm.

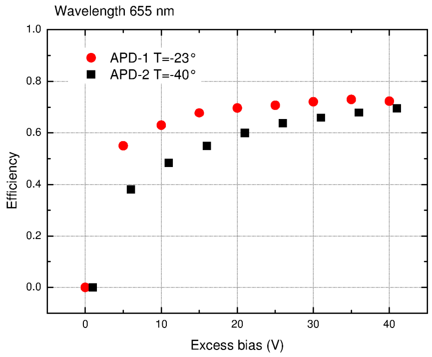

Figure 6: efficiency as a function of excess voltage measured at 655nm for both thick junction diodes

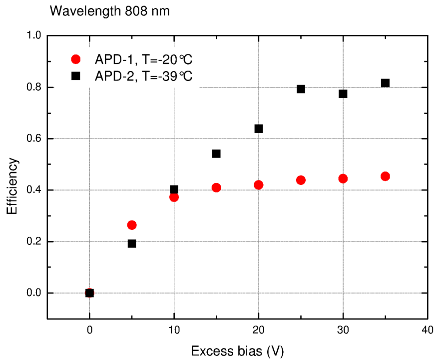

Figure 7: efficiency as a function of excess voltage measured at 808nm for both thick junction diodes

The shape of the detection gate of APD-2 for two values of the excess voltage is shown in figure 8. As can be seen the effective detection gate width is about 18ns when the electrical gate width is 20ns. This slight reduction is due to the rising and falling times (<2ns).

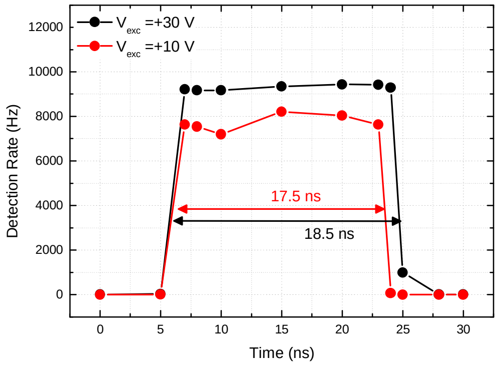

Figure 8: effective detection gate width measured for the APD-2 at two values of the excess voltage

The dark count probability values are presented in figure 9 as a function of the excess voltage. This probability is given per ns of effective gate. The efficiency values given in the graph correspond to the measurement performed at 655nm. Based on the two samples (one for each APD type) we measured that the noise of APD-1 is lower than the one of APD-2 even if APD-1 diode works at higher temperature. The noise probability value is 1.5e-6 per ns of effective gate for the APD-1 when the efficiency value is 64% at 655nm. The noise probability value is 6e-6 per ns of effective gate for the APD-2 when the efficiency value is 64% at 808nm.

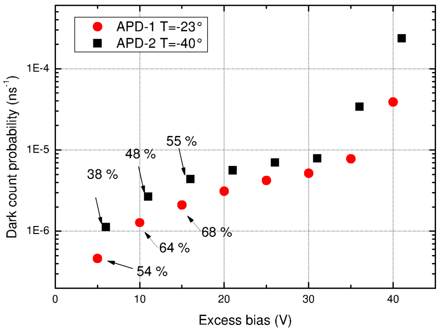

Figure 9: dark count probability as a function the excess voltage for both thick junction detectors

Similar measurements have been performed for the id110. The APD used in the id110 has a very thin junction compare to the two other diodes. That makes the id110 suitable for short wavelengths (~500nm). This is why it has also been calibrated at shorter wavelengths than the ones used for APD-1 and APD-2. The spectral response of the id110 is shown in figure 10. The maximal efficiency of this detector is within the range 500 to 600nm, where the efficiency value is about 24%. At this efficiency value, the noise probability is around 2e-6 per nanosecond of effective gate when the APD is cooled down to -40°C.

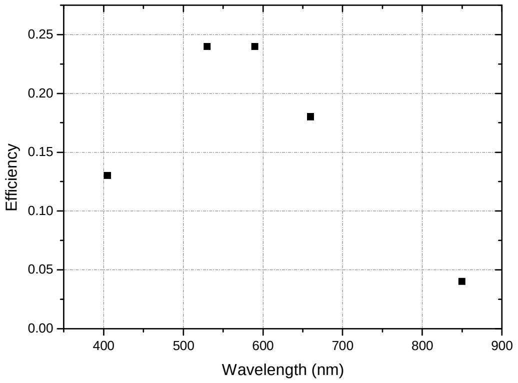

Figure 10: spectral response of the id110 in the range 400nm to 850nm

Charge persistence effect

In order to quantify the impact of the charge persistence effect, we simulate the scenario **B** by sending intense optical pulses on the detector and measuring the noise level as a function of the temporal delay from the arrival time of this intense pulse. Examples of the results of this kind of measurement are shown in figures 10 and 11. Figure 10 corresponds to a measurement performed with the APD-1 when we change the intensity of the optical pulse. Figure 11 shows the results obtained with the APD-2. In both cases, the frequency repetition rate is 100kHz and the APDs are cooled down to -20°C. As can be seen on both figures, the probability of having detection when the detector is activated while the photons impinge the detector is about 1. When the delay between the time of arrival of the photon and the time of activation of the detector is increased, the number of counts decreases but it is not equal to the dark count level. The additional noise comes from the charge persistence effect. For example, in figure 11, when the intense pulse contains 10 photons, the impact of the charge persistence effect is negligible after 50ns, whereas it is still important after 1us when the intense pulse contains at least 1000 photons. In figure 12, the charge persistence effect seems to be negligible after 50ns whatever the number of photons of the intense optical pulse is. However, the noise level of the APD-2 is much higher than the one of the APD-1, so it is difficult to compare quantitatively the charge persistence effect for the two diodes.

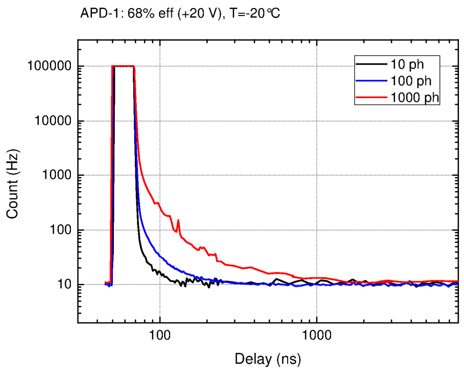

Figure 11: count rate of APD-1 as a function of the delay between the end of the rising edge of the gate and the laser pulse for several pulse energies.

It has to be noticed that a free-running detector based on the same APDs and a passive quenching circuit would have been blinded during the same period because of its dead time is about 1us. This demonstrates the advantage of the gated mode compare to the free-running mode in scenari **(a)** and **(b).** Indeed, the gated mode allows one to get a detector which has its highest efficiency value when the signal photon is arriving. The photons preceding the signal photon will just impact on the noise of the detector but not on its efficiency value. The larger the number of preceding photons the higher the charge persistence effect, so the higher the noise value.

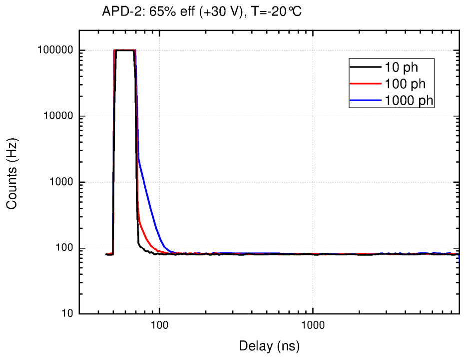

Figure 12: count rate of APD-2 as a function of the delay between the end of the rising edge of the gate and the laser pulse for several pulse energies.

The id110 is a module able to run in gated mode or in free-running mode. To demonstrate the advantages of the gated mode in scenari **(a)** and **(b)**, we measured the noise level after a strong illumination of the APD when it runs in both modes. The strong pulse intensity is of 1000 photons per pulse. The results of this measurement are shown in figure 13. For both measurements, the efficiency of the id110 was set at 22.3%. The relationship between efficiency and dark count probability is shown in figure14. Gate width of 20ns has been used when the module is running in gated mode. When the id110 module runs in free-running mode, a dead time of 70ns is applied. In order to get an integration time similar between the two measurements, we set the output signal of the id110 to 5ns and we count the coincidences with an electrical gate of about 10ns. For clarity of the chart, the delay values have been shifted by 100ns. It allows the use of logarithm scale for the x axis. As can be seen in figure 13, in gated mode, the id110 has roughly the same behaviour that the two thick junction APDs. The charge persistence effect disappears after about 100ns. On the contrary, in free-running mode, the detector is blinded during the 70ns dead time period (it looks a bit shorter on the graph because of the convolution with the output detector gate and the electrical gate used for coincidence). The noise is not equal to zero when the detector is blinded because there is a tiny probability that the detector was not active when the laser pulse arrived due to a dark count few tens of ns before. During the 70ns following the arriving of the laser pulse the efficiency in free-running mode has been estimated to be 6e-4 times smaller than the efficiency before the laser pulse arrives. This demonstrates that the gated mode allow one to keep a high efficiency when we activate the detector independently of the number of photons arriving before the signal (scenario **(a)** described in introduction). If we compare the charge persistence effect in both modes, we see that it is negligible after 100ns in gated mode, but it is still very important after 10us in free-running mode. So charge persistence effect has a stronger impact in free-running mode than in gated mode whereas the noise level is higher in free-running mode. This demonstrates the suitability of the gated mode in the scenario **(b).**

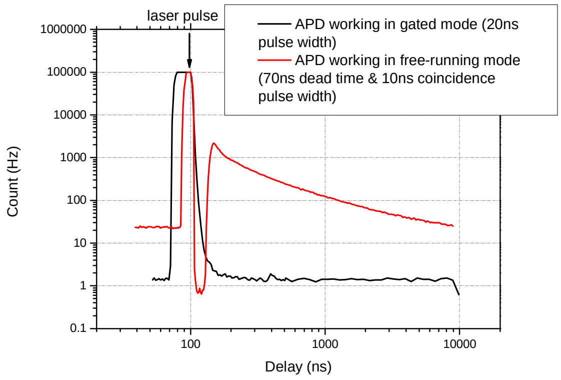

Figure 13: count rate of id110 as a function of the delay between the end of the falling edge of the gate and the laser pulse for several pulse energies. To allow the use of logarithmic scale, all delay values have been shifted by 100ns.

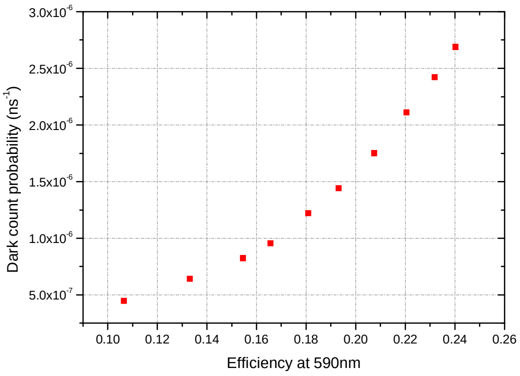

Figure 14: Dark count probability per nanosecond of effective gate. The optical signal used in this measurement has a wavelength of 590nm.

Conclusions

We presented two scenari where gated mode has a strong advantage to drive silicon APDs in Geiger mode compare to the standard passive quenching mode. The working of three types of Si-APDs has been shown with two different electrical circuits. The measurement of the noise level after the illumination of the diode by a more or less intense laser pulse demonstrated typical cases where gated mode is essential when high signal to noise ratio is crucial.

References

[1] S. Cova, M. Ghioni, A. Lotito, I. Rech, and F. Zappa, ”Evolution and prospects for single-photon avalanche diodes and quenching circuits”, J. of Mod. Opt. 51 , 1267-1288 (2004).

[2] A. Dalla Mora, A. Tosi, F. Zappa, S. Cova, D. Contini, A. Pifferi, L. Spinelli, A. Torri-celli, and R. Cubeddu, ”Fast-Gated Single-Photon Avalanche Diode for Wide Dynamic Range Near Infrared Spectroscopy”, Sel. Topics in Quant. El., IEEE, 16, 1023-1030 (2010).

[3] A. Tosi, A. Dalla Mora, F. Zappa, A. Gulinatti, D. Contini, A. Pifferi, L. Spinelli, A. Torricelli, and R. Cubeddu, ”Fast-gated single-photon counting technique widens dynamic range and speeds up acquisition time in time-resolved measurements”, Opt. Express, 19, 11, 10735-10746 (2011).

[4] .T. Lunghi, E. Pomarico, C. Barreiro, D. Stucki, B. Sanguinetti, and H. Zbinden, “Advantages of gated silicon single-photon detectors”, Appl. Opt., 51, 8455–8459 (2012)

[5] A. Lamas-Linares, C. Simon, J. C. Howell, and D. Bouwmeester, ”Experimental quantum cloning of single photons”, Science, 296, 712-714 (2002).

[6] N. Sangouard, B. Sanguinetti, N. Curtz, N. Gisin, R. Thew, and H Zbinden, ”Faithful Entanglement Swapping Based on Sum-Frequency Generation”, Phys. Rev. Lett., 106, 120403-1 - 120403-4(2011).

[7] A. Dalla Mora, D. Contini, A. Pifferi, R. Cubeddu, A. Tosi, and F. Zappa, ”Afterpulse-like noise limits dynamic range in time-gated applications of thin-junction silicon single-photon avalanche diode” Appl. Phys. Lett., 100, 241111-1 - 241111-4 (2012).

[8] J. Zhang, R. Thew, J. D. Gautier, N. Gisin, H. Zbinden, ”Comprehensive Characterization of InGaAs-InP Avalanche Photodiodes at 1550 nm With an Active Quenching ASIC”, Quant. Elect., IEEE Journ. of, 45, 792-799 (2009).

[9] P. Eraerds, M. Legre, J. Zhang, H. Zbinden, and N. Gisin, ”Photon Counting OTDR: Advantages and Limitations”, J. Lightwave Technol., 28, 952-964 (2010).

[10] N. Timoney, B. Lauritzen, I. Usmani, M. Afzelius, and N. Gisin ”Atomic frequency comb memory with spin wave storage in 153Eu3+:Y2SiO5”, submitted to J. Phys. B: At. Mol. Opt. Phys. (2012).

[11] ID Quantique, id210, available at: http://www.idquantique.com/images/stories/PDF/id210-single-photon-counter/id210-specs.pdf

[12] ID Quantique, id110, the spec sheet will be soon available on the website of ID Quantique: www.idquantique.com